

Microstructural evolution and magnetocaloric properties of off-stoichiometric $La_{1.2}Fe_{11.6}Si_{1.4}$ alloys with interstitial C atoms

Huiyan Zhang(张慧燕), Ye Zhu(朱叶), Fucheng Zhu(朱福成), Yang Xu(许旸), Yunbo Chen(陈云博), Hailing Li(李海玲), Weihua Gu(顾未华), Zhiyuan Liu(刘志愿), Weihuo Li(李维火), and Ailin Xia(夏爱林)

Citation: Chin. Phys. B, 2025, 34 (**8**): 088202. DOI: 10.1088/1674-1056/adce94
http://cpb.iphy.ac.cn; http://iopscience.iop.org/cpb

What follows is a list of articles you may be interested in

Electronic structure, elasticity, magnetism of Mn_2XIn(X =Fe, Co) full Heusler compounds under biaxial strain: First-principles calculations

Shiran Gao(皋世苒), Chengyang Zhao(赵成洋), Xinzhuo Zhang(张欣卓), Wen Qiao(乔文), Shiming Yan(颜士明), Ru Bai(白茹), and Tiejun Zhou(周铁军)

Chin. Phys. B, 2025, 34 (**1**): 017501. DOI: 10.1088/1674-1056/ad8ec5

Enhanced soft magnetic properties of SiO_2-coated FeSiCr magnetic powder cores by particle size effect

Mingyue Ge(葛铭悦), Likang Xiao(肖礼康), Xiaoru Liu(刘潇如), Lin Pan(潘嶙), Zhangyang Zhou(周章洋), Jianghe Lan(蓝江河), Zhengwei Xiong(熊政伟), Jichuan Wu(吴冀川), and Zhipeng Gao(高志鹏)

Chin. Phys. B, 2024, 33 (**10**): 107503. DOI: 10.1088/1674-1056/ad6556

Magnetic and magnetocaloric effect of $Er_{20}Ho_{20}Dy_{20}Cu_{20}Ni_{20}$ high-entropy metallic glass

Shi-Lin Yu(于世霖), Lu Tian(田路), Jun-Feng Wang(王俊峰), Xin-Guo Zhao(赵新国), Da Li(李达), Zhao-Jun Mo(莫兆军), and Bing Li(李昺)

Chin. Phys. B, 2024, 33 (**5**): 057502. DOI: 10.1088/1674-1056/ad1a94

Out-of-plane weak ferromagnetism at room temperaturein lattice-distortion non-collinear antiferromagnet of single-crystal Mn_3Sn

Bo-Xi Zhang(张博熙), Ping Song(宋平), Shan-Shan Deng(邓珊珊), Li Lou(娄理), and Sen Yao(姚森)

Chin. Phys. B, 2023, 32 (**8**): 087502. DOI: 10.1088/1674-1056/acca0b

Theoretical investigation on isomer formation probability and free energy of small C clusters

Lin Zheng-Zhe (林正喆)

Chin. Phys. B, 2015, 24 (**6**): 068201. DOI: 10.1088/1674-1056/24/6/068201

Microstructural evolution and magnetocaloric properties of off-stoichiometric $La_{1.2}Fe_{11.6}Si_{1.4}$ alloys with interstitial C atoms

Huiyan Zhang(张慧燕)[1,2,†], Ye Zhu(朱叶)[2], Fucheng Zhu(朱福成)[2], Yang Xu(许旸)[2], Yunbo Chen(陈云博)[2], Hailing Li(李海玲)[1,2], Weihua Gu(顾未华)[1,2], Zhiyuan Liu(刘志愿)[1,2], Weihuo Li(李维火)[2,3], and Ailin Xia(夏爱林)[1,2]

[1] *Advanced Ceramics Research Center, School of Materials Science and Engineering, Anhui University of Technology, Maanshan* 243002, *China*
[2] *School of Material Science and Engineering, Anhui University of Technology, Maanshan* 243002, *China*
[3] *Wuhu Technology and Innovation Research Institute, Anhui University of Technology, Wuhu* 241003, *China*

(Received 20 January 2025; revised manuscript received 31 March 2025; accepted manuscript online 21 April 2025)

This study investigated the effects of interstitial carbon doping on the microstructural and magnetocaloric properties of off-stoichiometric $La_{1.2}Fe_{11.6}Si_{1.4}C_x$ ($x = 0, 0.25, 0.5, 0.75, 1$) alloys. The alloys were prepared by melt-spinning following vacuum arc-melting. For the as-prepared and annealed samples, the carbon existed in the $La_2Fe_2Si_2C$ and $NaZn_{13}$-type La(Fe, Si)$_{13}$ (denoted by 1:13) phases, respectively. During the annealing process, the C atoms inhibited the diffusion reaction and depressed the generation of 1:13 phase, reducing mass fraction of the 1:13 phase in annealed $La_{1.2}Fe_{11.6}Si_{1.4}C_x$ compounds. The introduction of carbon resulted in lattice expansion and increased the Curie temperature (T_C) from 192 K to 273 K with $x = 0.5$. The first-order magnetic transition was gradually transformed into the second-order magnetic transition with increasing carbon content, which induced the significant reduction of thermal and magnetic hysteresis, as well as the maximum magnetic entropy change and adiabatic temperature change vary from 18.92 J/(kg·K) to 4.60 J/(kg·K) and from 4.9 K to 2.2 K under an applied field change of 0–2 T. The results demonstrate that interstitial carbon doping is an effective strategy to improve the magnetocaloric performance of La(Fe,Si)$_{13}$ alloys.

Keywords: interstitial C addition, off-stoichiometric La(Fe,Si)$_{13}$ alloy, magnetocaloric effect; magnetic transition

PACS: 82.30.Nr, 75.47.Np, 75.30.Sg, 75.30.Kz

DOI: 10.1088/1674-1056/adce94 **CSTR:** 32038.14.CPB.adce94

1. Introduction

Magnetic refrigeration (MR) based on magnetocaloric effect (MCE) is an alternative technology to conventional gas compression refrigeration, due to its advantages of environmental friendliness and high efficiency.[1–3] MCE refers to a reversable process that, when the external applied magnetic field changes the temperature of magnetic materials varies, under the adiabatic condition.[4] The development of near room-temperature MR started in 1976 by Brown,[5] he utilized rare earth metal Gd (with the Curie temperature, T_C, of 293 K) to build the first room-temperature magnetic refrigerator prototype successfully, under an applied magnetic field range of 0–7 T, the maximum magnetic entropy change ($|\Delta S_M^{max}|$) of 13.2 J/(kg·K) was observed. However, owing to the low MCE and high cost of Gd, the giant MCE (GMCE) materials, such as $Gd_5(Si_{1-x}Ge_x)_4$,[6] MnAs-based compounds,[7] Ni–Mn-based Heusler alloys,[8] and La(Fe,Si)$_{13}$ series alloys,[9] were successively discovered.

In the most recent refrigerator prototypes, La(Fe,Si)$_{13}$ with an fcc $NaZn_{13}$-type structure (1:13 phase, $Fm\bar{3}c$ space group), as one of the most used refrigerant for room temperature range, attracted more attention with merits of low cost, abundant raw materials, adjustable T_C, and large magnetic entropy change ($|\Delta S_M|$).[1,2,10] The $LaFe_{13-x}Si_x$ ($1.0 \leq x \leq 1.6$) compounds exhibit the GMCE, which results from their first-order magnetic transition (FOMT) accompanied by itinerant electron metamagnetic transition (IEMT).[3] The main obstacles in the practical applications of this kind of material include the low T_C, large thermal and magnetic hysteresis and long annealing time to obtain the 1:13 phase.[11] To raise the T_C, several achievements have been attained through changing the Fe/Si mass ratio, replacing Fe by Co and doping with interstitial atoms (C, H, B, N).[2] For instance, in $LaFe_{13-x}Si_x$ ($x = 1$, 1.2, 1.43, 1.6, 1.8) alloy ribbons,[12] their T_C rises with increasing x, but the $|\Delta S_M^{max}|$ decreases dramatically, which is ascribed to the loss of IEMT; moreover, the T_C only reaches 231 K for relatively high contents of Si ($x = 1.8$), indicating there is a limitation to increase the T_C using this method. Chen[13] *et al.* reported that the T_C of $LaFe_{11.6-x}Co_xSi_{1.4}$ shifted from 207 K to 285 K by substituting Co for Fe from $x = 0.1$ to $x = 0.08$, while the $|\Delta S_M|$ and hysteresis were reduced as a result of the change from FOMT occurring in the material to the second-order magnetic transition (SOMT).

Introduction of interstitial atoms can extend the distance

†Corresponding author. E-mail: hyzh2017@ahut.edu.cn

© 2025 Chinese Physical Society and IOP Publishing Ltd. All rights, including for text and data mining, AI training, and similar technologies, are reserved.

of Fe–Fe coupling and then weakens the overlap of the Fe-3d wave functions, which leads to the enhancement of Fe–Fe exchange interaction and increasement of the T_C.[14,15] Intrusion of hydrogen at 24d interstitial sites in 1:13 phase is the only way that can adjust the T_C to near room temperature without sacrificing the MCE (maintaining the FOMT).[2] Furthermore, the thermal and magnetic hysteresis of hydrogenated La(Fe,Si)$_{13}$ decreases remarkably. The main shortcoming of these hydrides is instability, which will deteriorate MCE.[16,17] Previous studies have shown that B atoms can dissolve in α-Fe, partially react with Fe to form Fe_2B, and typically occupy 24d interstitial sites or 96*i* Fe/Si substitutional sites in 1:13 phase.[15,18] Therefore, the improvement of magnetocaloric performance through B doping is limited, although the $|\Delta S_M|$ of $La_{1.2}Fe_{11.6}Si_{1.4}B_{0.75}$ is larger than that of $La_{1.2}Fe_{11.6}Si_{1.4}$, the increment of T_C is only 7 K.[19] The interstitial C was expected to be an alternative to H, and with increasing C content, the T_C of $LaFe_{11.6}Si_{1.4}C_x$ ($x = 0$–0.6) rises from 195 K to 250 K, however the transition of FOMT to SOMT was observed, which results in noticeable reduction of their MCE.[20]

To shorten the annealing time for obtaining the 1:13 phase, the most commonly approach is producing the alloys by melt-spinning technology (with high cooling rate), because the refined crystalline microstructure is beneficial to the atomic diffusion.[21] Moreover, the high cooling rate contributes to the depression of thermal and magnetic hysteresis.[22] The composition also affects the annealing process, e.g., the existence of excessive La in off-stoichiometric $La_{1+x}Fe_{11.6}Si_{1.4}$ ($x = 0$–1.2) alloys can modify the microscopic morphology of the as-spun ribbons and accelerate the formation rate of 1:13 phase.[23]

In the researches about introducing interstitial C into stoichiometric La(Fe,Si)$_{13}$ compounds, when the content of C exceeds $x = 0.6$ in $LaFe_{11.6}Si_{1.4}C_x$[20] and $LaFe_{11.5}Si_{1.5}C_x$,[24,25] the addition of C is unfavorable for the formation of 1:13 phase and the amount of residual α-Fe increases. To explore whether the modified microstructure in off-stoichiometric $La_{1+x}Fe_{11.6}Si_{1.4}$ alloys can promote the concentration of interstitial C and the T_C any further, this study prepared a series of $La_{1.2}Fe_{11.6}Si_{1.4}C_x$ ($x = 0$, 0.25, 0.5, 0.75, 1) compounds with different C contents through melt-spinning method, and investigated the influence of doping C on their microstructural, magnetic and magnetocaloric properties.

2. Experimental details

The ingots with nominal composition of $La_{1.2}Fe_{11.6}Si_{1.4}C_x$ ($x = 0$, 0.25, 0.5, 0.75, 1) were prepared by vacuum arc-melting in high purity argon atmosphere. The purity of the metals used is 99.9 wt% for La, 99.95 wt% for Fe, 99.99 wt% for Si, and 99.9 wt% for pre-alloyed Fe–C (the mass ratio of Fe/C is 95/5). In order to ensure the composition uniformity of the alloy, the ingots were turned over and remelted for five times. The pieces of ingot were put into a quartz tube with a nozzle, and the ribbons were fabricated by melt-spinning with a rolling copper wheel (the surface linear velocity of 20 m/s) under protection of high purity argon atmosphere. Then the ribbons were encapsulated in a vacuum quartz tube and annealed at 1323 K for 2 h, followed by furnace cooling down to room-temperature. Part of the as-spun and annealed ribbons were grinded into powder for characterization.

The x-ray diffractometer (XRD, Rigaku Ultima IV) with Cu K_α radiation ($\lambda = 0.154178$ nm) in the 2θ range of 20°–90° was used to examine the phase structure of the samples. The Rietveld refinement of the XRD pattern was applied using an FULLPROF software for quantitative phase analysis and observing lattice parameters.[26] Microstructure was detected by scanning electron microscopy (SEM, JEOL JEM-6480) equipped with the energy dispersive spectrometer (EDS). The room temperature magnetic hysteresis loops were detected by a vibrating sample magnetometer (VSM, Microsense EZ7). Magnetic property measurement system (MPMS, Quantum Design MPMS 3) with the SQUID (superconducting quantum interference device) magnetometer was utilized to measure the following magnetic properties. The temperature dependence of magnetization (M–T) curves were detected during zero-field-cooled (ZFC) heating and field-cooled (FC) cooling processes under an applied field of 0.02 T. The isothermal magnetization (M–H) curves were collected under the magnetic field changing from 0 T to 2 T at different selected temperatures, and the temperature interval was chosen as 2 K in vicinity of T_C and 5 K away from T_C, respectively. Under the condition of zero magnetic field, the specific heat capacity was tested by differential scanning calorimetry (DSC, Netzsch DSC 204 F1) with sapphire as the reference material, and the heating rate was retained at 10 K/min.

3. Results and discussion

Figure 1 shows the XRD patterns of $La_{1.2}Fe_{11.6}Si_{1.4}C_x$ ($x = 0$, 0.25, 0.5 0.75, 1) alloys before and after annealing. As displayed in Fig. 1(a), the main phase of as-prepared $La_{1.2}Fe_{11.6}Si_{1.4}C_x$ alloys is α-Fe ($Im\bar{3}m$ space group), and the secondary phase in samples with and without C addition are identified to be LaFeSi ($P4/nmm$ space group), and $La_2Fe_2Si_2C$ ($C2/m$ space group),[27] respectively. From local magnification of the XRD patterns in Fig. 1(c), it can be seen the main peak of α-Fe phase is not shifted after adding C, indicating the C atoms preferred to enter the lattice of LaFeSi rather than dissolved in α-Fe, and finally formed the $La_2Fe_2Si_2C$ compound. This phenomenon is probably attributed to the stronger chemical bonding of La–C atomic pair than that of Fe–C atomic pair.[28,29] Similarly, in the unannealed $LaFe_{11.5}Si_{1.5}C_x$ ($x = 0$, 0.1, 0.2, 0.3) alloys, C atoms

exist in interstitial sites of La(Fe, Si)$_{13}$ phase other than in α-Fe phase.[25,28]

In present work, the annealed $La_{1.2}Fe_{11.6}Si_{1.4}C_x$ ($x = 0$, 0.25, 0.5 0.75, 1) alloys contain the main phase $NaZn_{13}$-type 1:13 ($Fm\bar{3}c$ space group) and the residual α-Fe, as exhibited in Fig. 1(b). From Figs. 1(d) and 1(e), the locally magnified XRD pattern, it can be observed that with the addition of C, the peaks of the 1:13 phase shift towards lower angle, whereas the peaks of Fe are almost unchanged, demonstrating the C atoms are dissolved in the 1:13 phase and probably occupy the 24d interstitial sites of the lattice.[18,28] It can be confirmed by the results from the Rietveld refinement of the XRD spectra listed in Table 1. The enlarged lattice parameters of 1:13 phase with addition of C means the carbonization expands the unit cell. Therefore, during the heat treatment, the peritectoid reaction occurred in these samples should be: α-Fe + LaFeSi (or $La_2Fe_2Si_2C$) = La(Fe, Si)$_{13}$(C).[23,30] On the other aspect, the amount of residual α-Fe phase increases with the concentration of carbon, resulting in the reduction of relative weight fraction of 1:13 phase. Introduction of carbon possibly hinders the diffusion reaction between α-Fe and $La_2Fe_2Si_2C$, thereby suppressing the formation of 1:13 phase.[23,31]

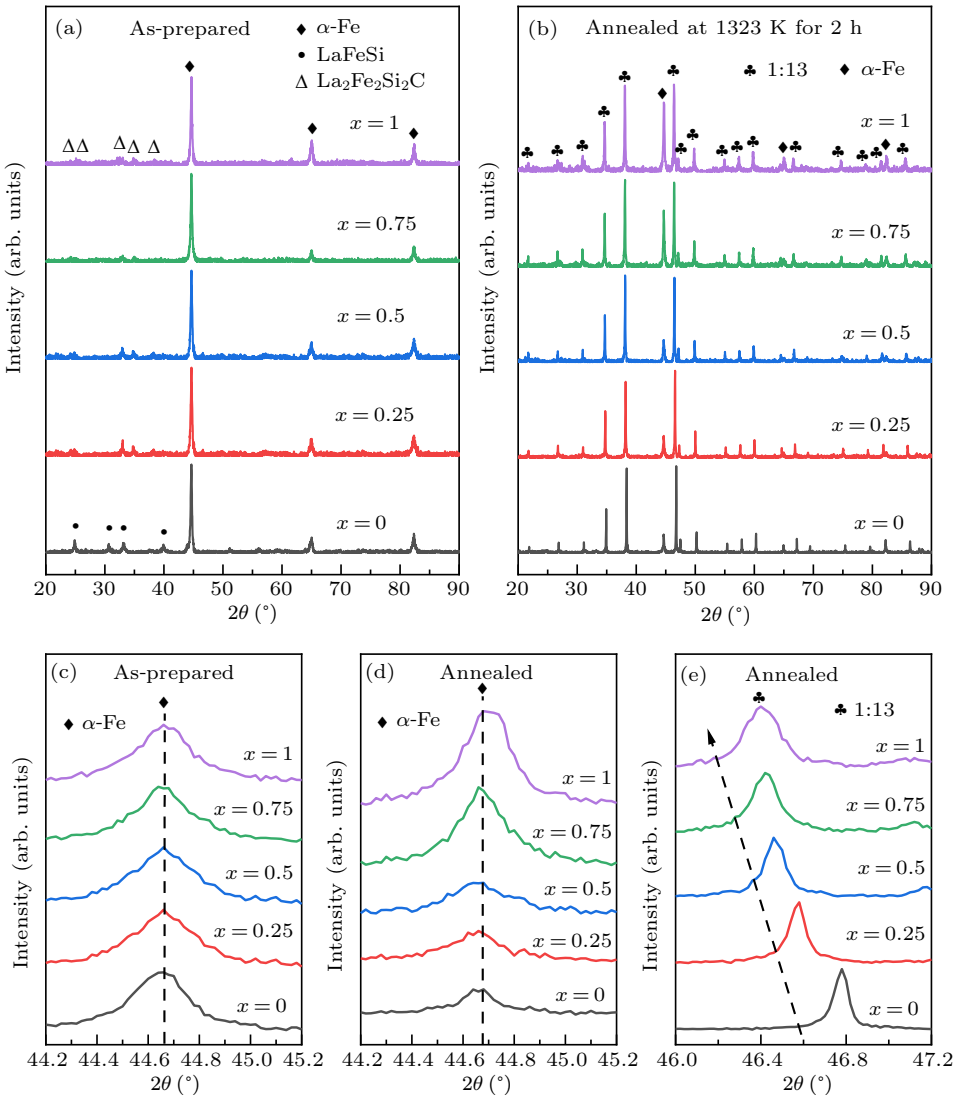


Fig. 1. XRD patterns of $La_{1.2}Fe_{11.6}Si_{1.4}C_x$ alloys in the (a) as-prepared and (b) annealed states. Panels (c), (d), and (e) are localized magnified XRD patterns of panels (a) and (b), respectively.

Table 1. The phase fraction and lattice parameters of 1:13 phase and α-Fe in the annealed $La_{1.2}Fe_{11.6}Si_{1.4}C_x$ compounds, as well as the reliability factors R_{wp}, R_{exp}, and χ^2.

Sample	1:13 phase		α-Fe phase		R_{wp}	R_{exp}	χ^2
	Mass fraction (wt%)	$a = b = c$ (Å)	Mass fraction (wt%)	$a = b = c$ (Å)			
$x = 0$	84.45	11.4749	15.55	2.8660	8.21	7.63	1.61
$x = 0.25$	80.11	11.5145	19.89	2.8644	7.81	7.70	1.03
$x = 0.5$	79.52	11.5354	20.48	2.8631	8.09	7.66	1.12
$x = 0.75$	73.54	11.5537	26.46	2.8636	8.13	7.30	1.24
$x = 1$	68.96	11.5641	31.04	2.8646	8.36	7.37	1.29

Figure 2(a) displays the room-temperature magnetic hysteresis loops of the $La_{1.2}Fe_{11.6}Si_{1.4}C_x$ samples after annealing, and the saturated magnetization M_S is 22.78, 31.25, 45.94, 74.64, and 87.84 A·m^2/kg corresponding to $x = 0$, 0.25, 0.5, 0.75, 1, respectively. At room-temperature, α-Fe phase is ferromagnetic while 1:13 phase is paramagnetic; therefore, the smaller M_S value indicates the less relative content of α-Fe phase. With doping of carbon, the amount of residual α-Fe phase increases, which is generally consistent with above analysis of XRD results.

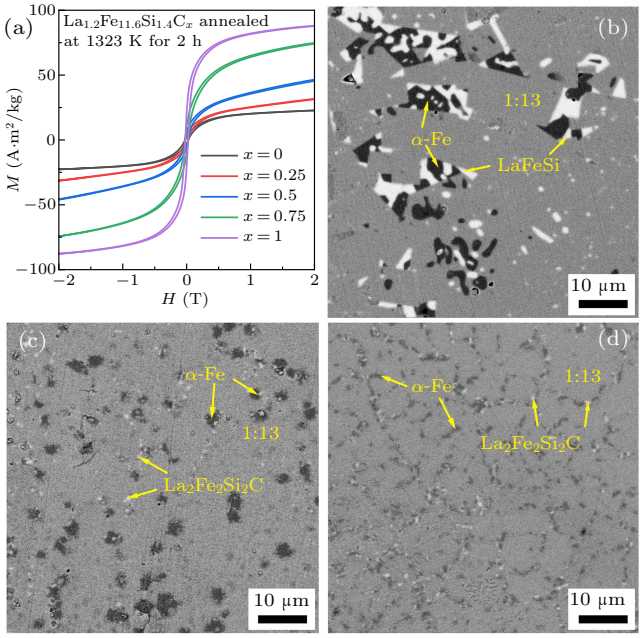


Fig. 2. (a) Room-temperature magnetic hysteresis loops of the annealed $La_{1.2}Fe_{11.6}Si_{1.4}C_x$ compounds, and the SEM images for samples with (b) $x = 0$, (c) $x = 0.25$, (d) $x = 0.5$ in BSE mode.

In La(Fe,Si)$_{13}$ alloys, the magnetocaloric effect is induced by the 1:13 phase. Therefore, the fraction of the 1:13 phase plays a critical role in regulating the magnetocaloric properties of the alloy. As reported in previous study,[32] for $LaFe_{11.8}Si_{1.2}$ the $|\Delta S_M^{max}|$ (under magnetic field change of 2 T) dropped down remarkably from $\sim$ 24.3 J/(kg·K) to $\sim$ 7.0 J/(kg·K) as the amount of 1:13 phase decreased from $\sim$ 90% to $\sim$ 57.5%. Therefore, the subsequent research focuses on the $La_{1.2}Fe_{11.6}Si_{1.4}C_x$ alloys with $x = 0$, 0.25 and 0.5 due to their relatively high mass fraction of the 1:13 phase. Figures 2(b)–2(d) present the SEM images of annealed $La_{1.2}Fe_{11.6}Si_{1.4}C_x$ in backscattered electron (BSE) mode. According to the EDS measurement, the gray matrix, black area and white part are the 1:13, α-Fe and La-rich phases, respectively. Because of the low amount of La-rich phase, it was not detected by XRD. In addition, regardless of the compound contains carbon or not, the content ratio of La, Fe, and Si is 1:1:1 in the La-rich phase (LaFeSi or $La_2Fe_2Si_2C$). The α-Fe and La-rich phases with distinct grain boundaries in Fig. 2(b), are randomly distributed in various parts as small islands after the introduction of C atoms (shown in Figs. 2(c) and 2(d)). With the addition of C, the alloy undergoes grain refinement. Usually, grain refinement promotes the atomic diffusion and formation of the 1:13 phase,[21] whereas in this study the C atoms located in the $La_2Fe_2Si_2C$ phase probably inhibit the diffusion reaction between α-Fe and $La_2Fe_2Si_2C$.[23,31]

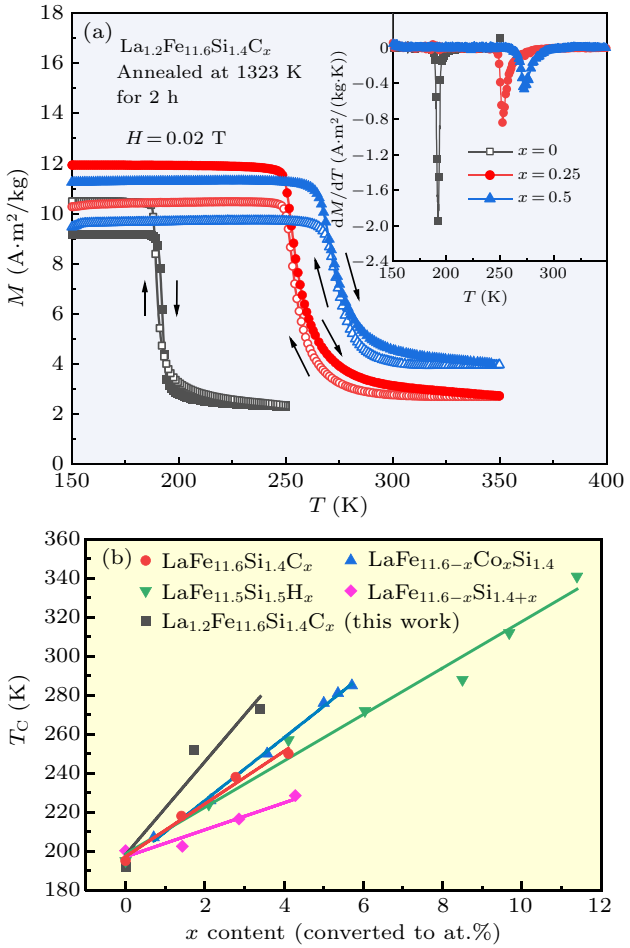


Fig. 3. (a) The M–T curves under a magnetic field of 0.02 T (detected during ZFC heating and FC cooling processes) for $La_{1.2}Fe_{11.6}Si_{1.4}C_x$ ($x = 0$, 0.25, 0.5) samples, and the insert is their dM/dT *versus* T plots derived from the ZFC M–T curves. (b) Correlation of the T_C with elemental content in $La_{1.2}Fe_{11.6}Si_{1.4}C_x$ and some other series of La(Fe, Si)$_{13}$ alloys (the data taken from Refs. [13,20,37,38]). Lines are guides to display the trend after adding corresponding elements.

Figure 3(a) exhibits the ZFC-heating and FC-cooling M–T curves of $La_{1.2}Fe_{11.6}Si_{1.4}C_x$ ($x = 0$, 0.25, 0.5) alloys under the applied field of 0.02 T. Manifest FM–PM transition is obtained in all the samples near their T_C, which is defined as the temperature corresponding to minimum value of derivative dM/dT of the ZFC-heating M–T curves[33] (illustrated in the inset of Fig. 3(a)). The magnetization of the alloys is not close to zero at the temperature higher than T_C, owing to the existence of α-Fe. When $x = 0$, 0.25, and 0.5, the T_C is 192, 252, and 273 K, respectively, increasing with addition of carbon. The lattice expansion resulted from the intrusion of interstitial carbon reduces the overlap of the Fe-3d wave functions and enhances the Fe–Fe exchange interaction, which induces the increase of T_C.[34] The T_C of $La_{1.2}Fe_{11.6}Si_{1.4}$ in

present study is higher than the values of 184 K and 177 K reported previously,[19,23] probably attributed to its higher Si/Fe ratio content of 1:13 phase.[35,36] Moreover, the thermal hysteresis was calculated by the difference between the transition temperature obtained from the heating and cooling M–T curves,[33] and the values are 2.95 K, 0.2 K, and nearly zero for the samples with $x = 0$, 0.25, and 0.5, respectively. It is noticeable the thermal hysteresis was significantly reduced after carbonized.

As mentioned in Section 1, replacement of Fe by Si or Co and intrusion of interstitial C or H in La(Fe, Si)$_{13}$ alloys are effective strategy to raise their T_C. Figure 3(b) manifests the nearly linear variation of the T_C with composition for different series of La(Fe, Si)$_{13}$ alloys, each 1 at.% augmentation of C, H, Co, and Si makes the T_C of $La_{1.2}Fe_{11.6}Si_{1.4}C_x$ (this research), $LaFe_{11.6}Si_{1.4}C_x$,[20] $LaFe_{11.5}Si_{1.5}H_x$,[37] $LaFe_{11.6-x}Co_xSi_{1.4}$[13] and $LaFe_{13-x}Si_x$[38] go up by 23.9 K, 13.5 K, 11.9 K, 16.1 K, and 6.9 K, respectively. The addition of carbon in off-stoichiometric $La_{1.2}Fe_{11.6}Si_{1.4}C_x$ improves the T_C a larger increment, which is possibly ascribed to the excessive La attracting more C atoms around it, followed by the enhanced lattice expansion.

The isothermal magnetization and demagnetization (M–H) curves of $La_{1.2}Fe_{11.6}Si_{1.4}C_x$ ($x = 0$, 0.25, 0.5) under the applied field change of 0 T–2 T are depicted in Figs. 4(a)–4(c). The $La_{1.2}Fe_{11.6}Si_{1.4}$ undoped with carbon exhibits abrupt changes of magnetization above the critical field and obvious hysteresis loops, while the magnetic hysteresis of $La_{1.2}Fe_{11.6}Si_{1.4}C_{0.25}$ and $La_{1.2}Fe_{11.6}Si_{1.4}C_{0.5}$ are neglectable. The magnetic hysteresis is mainly due to the field-induced first-order IEMT from PM to FM state above T_C, which can be estimated by the area enclosed by the ascending and descending magnetization curves,[15] and the maximum value of magnetic hysteresis loss near T_C is 13.24 J/kg for $La_{1.2}Fe_{11.6}Si_{1.4}$. Additionally, the residual α-Fe phase leads to the nonlinear M–H curves at temperatures much higher than T_C.[12]

The nature of magnetic transition can be determined by the Arrott (M^2–H/M) plots. Figure 4(d) illustrates the Arrott plots calculated by M–H data of the $La_{1.2}Fe_{11.6}Si_{1.4}C_x$ ($x = 0$, 0.25, 0.5) compounds just above their T_C. The negative slope and "S" shape with an inflection point of the curve for $La_{1.2}Fe_{11.6}Si_{1.4}$ confirms the first-order magnetic transition, while the positive slope and monotonical increase of the curves for $La_{1.2}Fe_{11.6}Si_{1.4}C_{0.25}$ and $La_{1.2}Fe_{11.6}Si_{1.4}C_{0.5}$ indicates the second-order magnetic transition. Therefore, the addition of C atoms changes the magnetic transition in $La_{1.2}Fe_{11.6}Si_{1.4}C_x$ from FOMT to SOMT, which is accordance with the remarkable reduction of thermal and magnetic hysteresis. Previously, similar results for $LaFe_{11.6}Si_{1.4}C_x$ alloys have been reported.[20]

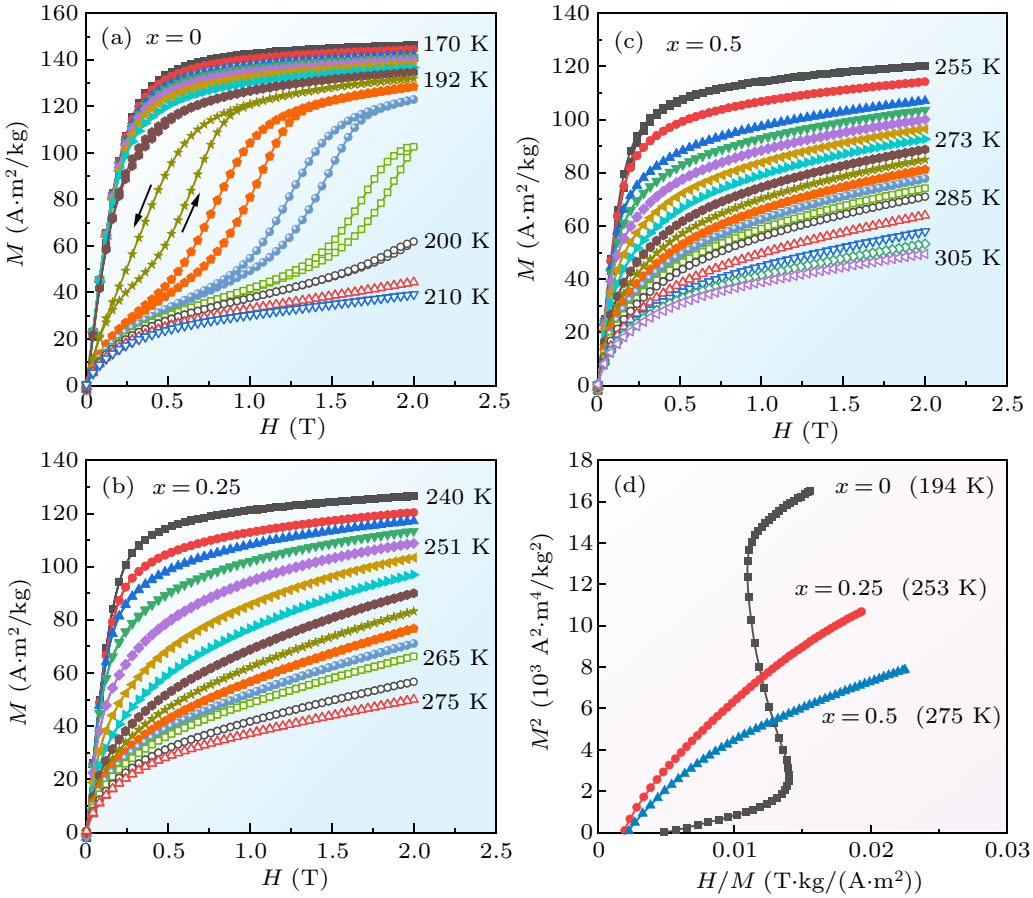


Fig. 4. (a)–(c) Magnetization isotherms of the annealed $La_{1.2}Fe_{11.6}Si_{1.4}C_x$ ($x = 0$, 0.25, 0.5) alloys measured at various temperatures in vicinity of T_C under the increasing and decreasing magnetic field of 0 T–2 T. (d) Arrott curves at the temperature near their T_C.

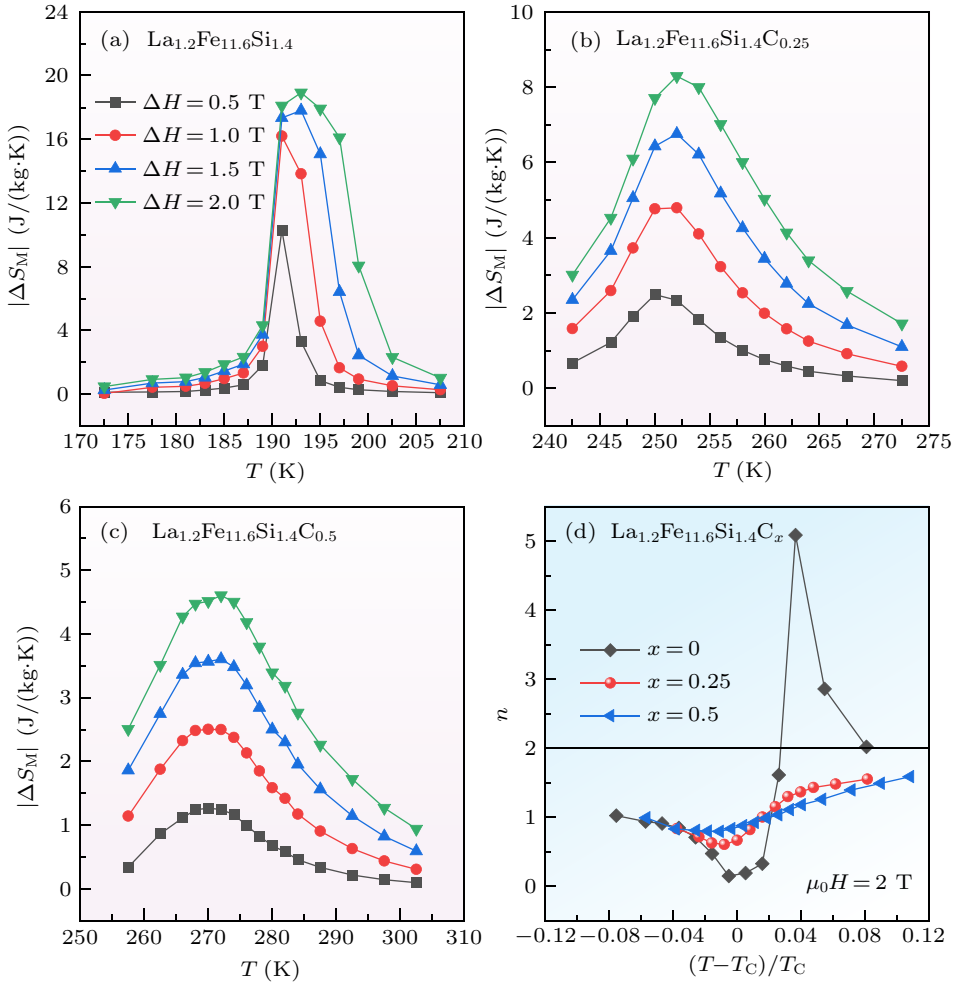


Fig. 5. The $|\Delta S_M|$–T curves of annealed $La_{1.2}Fe_{11.6}Si_{1.4}C_x$ samples with (a) $x = 0$, (b) $x = 0.25$, (c) $x = 0.5$ under the ΔH of 0.5, 1.0, 1.5, and 2 T. (d) Temperature dependence of exponent n curves under a magnetic field of 2 T.

To evaluate the magnetocaloric effect of annealed $La_{1.2}Fe_{11.6}Si_{1.4}C_x$ ($x = 0$, 0.25, 0.5) alloys, the isothermal magnetic entropy change (ΔS_M) was calculated from the M–H curves by the Maxwell equation[39] and its numerical approximation[40]

$$\begin{aligned}\Delta S_M(T,H) &= S_M(T,H) - S_M(T,0) \\ &= \int_0^H \left\{\frac{\partial M(T,H)}{\partial T}\right\}_H \mathrm{d}H, \qquad (1)\end{aligned}$$

$$\Delta S_M\left(\frac{T_{i+1}+T_i}{2}\right) = \sum_i \frac{M_{i+1}-M_i}{T_{i+1}-T_i}\Delta H_i, \qquad (2)$$

where M_i and M_{i+1} are experimental data of magnetization at temperatures of T_i and T_{i+1}, respectively, under the magnetic field of H_i. Figure 5 shows the temperature dependent $|\Delta S_M|$ under various applied field changes (ΔH). There is still some controversy about using the Maxwell equation to determine the $|\Delta S_M|$ of the FOMT materials. In some reports,[41,42] the resulting $|\Delta S_M|$ was overestimated and a spurious peak was obtained near the T_C. In this study, the symmetrical $|\Delta S_M|$–T curves without spurious $|\Delta S_M|$ peaks reflect the reliability in estimating the magnetocaloric effect.[43] For the $La_{1.2}Fe_{11.6}Si_{1.4}C_x$ with $x = 0$, 0.25, 0.5, the maximum magnetic entropy change $|\Delta S_M^{max}|$ of 18.92, 8.29, and 4.60 J/(kg·K) were observed at 193 K, 252 K, and 272 K (near their T_C), respectively, under $\Delta H = 2$ T. The introduction of C atoms suppresses the first-order IEMT in the alloys, therefore the $|\Delta S_M^{max}|$ decreases. The relation between the $|\Delta S_M^{max}|$ ($\Delta H = 2$ T) and the T_C of $La_{1.2}Fe_{11.6}Si_{1.4}C_x$ (this study), $LaFe_{11.6}Si_{1.4}C_x$,[44] $La(Fe_{0.88}Si_{0.12})_{13}H_x$,[36] $LaFe_{11.6-x}Co_xSi_{1.4}$,[13] and $LaFe_{13-x}Si_x$[38] were presented in Fig. 6. As T_C was tuned to higher temperature, the transition gradually changes from FOMT to SOMT and the $|\Delta S_M^{max}|$ drops considerably for these series of alloys except $La(Fe_{0.88}Si_{0.12})_{13}H_x$, which retains FOMT after hydrogenated. These declining tendencies in $La_{1.2}Fe_{11.6}Si_{1.4}C_x$ and $LaFe_{11.6-x}Co_xSi_{1.4}$ are similar and less drastic than that in $LaFe_{13-x}Si_x$ and $LaFe_{11.6}Si_{1.4}C_x$, indicating the addition of carbon (lower cost than Co and more stable than hydrogenation) in off-stoichiometric La-excessive La_{1+x} (Fe, Si)$_{13}$ alloys is a proposed approach to develop near room-temperature magnetic refrigerant.

The field dependence of $|\Delta S_M|$ follows the power law of $|\Delta S_M| \propto H^n$, and the temperature and field dependent exponent

n can be locally evaluated by the equation:

$$n(T,H) = \frac{\mathrm{d}\ln|\Delta S_{\mathrm{M}}|}{\mathrm{d}\ln H}. \tag{3}$$

The detection of $n > 2$ after the magnetic transition is a criterion to determine that the transition is an FOMT.[45] From the correlation between n and temperature for $La_{1.2}Fe_{11.6}Si_{1.4}C_x$ alloys under a magnetic field of 2 T plotted in Fig. 5(d), it can be found that the n reached the minimum near the T_{C} of each sample, then it achieved a value larger than 2 only for $La_{1.2}Fe_{11.6}Si_{1.4}$. These results demonstrate the magnetic transition of $La_{1.2}Fe_{11.6}Si_{1.4}$ is FOMT, while those of $La_{1.2}Fe_{11.6}Si_{1.4}C_{0.25}$ and $La_{1.2}Fe_{11.6}Si_{1.4}C_{0.5}$ are SOMT, which is consistent with the estimation from Arrott plots.

Another parameter for evaluating the magnetocaloric performance of magnetic materials is the refrigeration capacity (RC), which reflects the heat transfer between the cold and hot reservoirs in an ideal refrigerant cycle.[2] Specifically, RC_{AERA} and RC_{FWHM} are defined as $RC_{\mathrm{AREA}} = \int_{T_{\mathrm{cold}}}^{T_{\mathrm{hot}}} \Delta S_{\mathrm{M}}^{\max} \mathrm{d}T$ and $RC_{\mathrm{FWHM}} = |\Delta S_{\mathrm{M}}^{\max}| \times \Delta T_{\mathrm{FWHM}}$, respectively, where T_{cold} and T_{hot} are the temperatures of the reservoirs. Conventionally, the temperature span between the reservoirs is approximated by the full width at half maximum of the peak, ΔT_{FWHM}. The values of RC_{FWHM} ($\Delta H =$ 2 T) for $La_{1.2}Fe_{11.6}Si_{1.4}C_x$ are 168.4 J/kg, 139.9 J/kg, and 141.6 J/kg when $x = 0$, 0.25 and 0.5, respectively. Although the addition of C reduced the RC_{FWHM} by approximately 16%–17%, the working temperature range was remarkably widened from 8.90 K to 30.78 K. The magnetocaloric properties of the $La_{1.2}Fe_{11.6}Si_{1.4}C_x$ compounds and several representative materials (with similar working temperature) are listed in Table 2. For both stoichiometric $LaFe_{11.6}Si_{1.4}C_x$ and off-stoichiometric $La_{1.2}Fe_{11.6}Si_{1.4}C_x$, the introduction of C raised the T_{C} and lowered the $|\Delta S_{\mathrm{M}}^{\max}|$. Compared to other magnetic refrigeration materials with similar T_{C} (including $LaFe_{11.6}Si_{1.4}C_{0.4}$), the $La_{1.2}Fe_{11.6}Si_{1.4}C_{0.25}$ and $La_{1.2}Fe_{11.6}Si_{1.4}C_{0.5}$ alloys have advantages of large magnetic entropy change, wide working temperature range, high refrigeration capacity, and low cost. These characteristics make them promising candidates for near-room-temperature magnetic refrigerator technology.

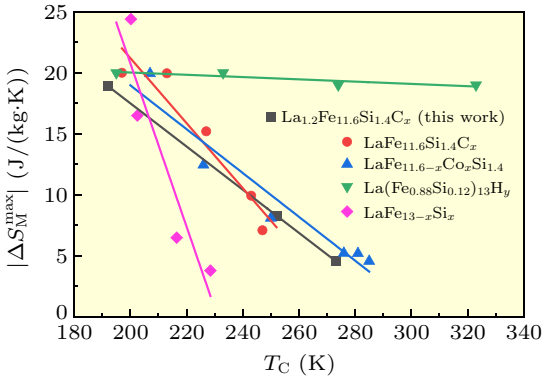


Fig. 6. Relation between $|\Delta S_{\mathrm{M}}^{\max}|$ and T_{C} of $La_{1.2}Fe_{11.6}Si_{1.4}C_x$ and some other series of La(Fe, Si)$_{13}$ alloys (the data taken from Refs. [13,36,38,44]). Solid lines aim to depict the varying tendency caused by introducing the corresponding elements.

Table 2. Magnetocaloric properties of present alloys and some representative magnetic refrigeration materials.

Materials	T_{C} (K)	$\lvert\Delta S_{\mathrm{M}}^{\max}\rvert$ (J/(kg·K))	ΔT_{FWHM} (K)	RC_{FWHM} (J/kg)	RC_{AERA} (J/kg)	Reference
$La_{1.2}Fe_{11.6}Si_{1.4}$	192	18.92	8.90	168.4	146.21	this work
$La_{1.2}Fe_{11.6}Si_{1.4}C_{0.25}$	252	8.29	16.87	139.9	108.73	this work
$La_{1.2}Fe_{11.6}Si_{1.4}C_{0.5}$	273	4.60	30.78	141.6	109.10	this work
$LaFe_{11.6}Si_{1.4}$	195	~ 20.02	~ 10	~ 200.2	~ 175.07	[44]
$LaFe_{11.6}Si_{1.4}C_{0.2}$	227	~ 15.57	~ 10.78	~ 167.84	~ 138.12	[44]
$LaFe_{11.6}Si_{1.4}C_{0.4}$	248	~ 7.19	~ 21.91	~ 157.5	~ 118.63	[44]
$LaFe_{11.5}Si_{1.5}C_{0.5}$	241	~ 7.55	~ 20.29	~ 153.2	~ 115.17	[34]
$LaFe_{11.1}Co_{0.5}Si_{1.4}$	250	8.10	~ 14.4	~ 116.6	~ 89.97	[13]
$LaFe_{10.9}Co_{0.7}Si_{1.4}$	276	5.21	~ 23.36	~ 121.7	~ 95.1	[13]
$La_{0.7}Ca_{0.3}MnO_3$	251	~ 5.71	~ 14.47	~ 82.6	~ 68.4	[46]
$La_{0.67}Ca_{0.33}MnO_3$	278	4.33	–	86.6	–	[47]
Gd	292	5.20	–	226.9	~ 171.3	[48]

However, the RC is not sufficient to compare the quality of magnetocaloric materials, since it often overestimates the operating temperature range of the materials with a broad and short $|\Delta S_{\mathrm{M}}|$ peak.[2,48] The parameter also ignores the importance of the adiabatic temperature change (ΔT_{ada}).[48,49] In this work, the ΔT_{ad} was calculated by combined data of zero field heat capacity C_{p} (0, T) and $|\Delta S_{\mathrm{M}}|$ (observed from M–H data) through the following relation:[50]

$$S(0,T) = \int_{T_1}^{T_2} \frac{C_{\mathrm{p}}(0,T)}{T} \mathrm{d}T, \tag{4}$$

$$S(H,T) = \Delta S_{\mathrm{M}} + S(0,T), \tag{5}$$

where $S(0,T)$ and $S(H,T)$ are the temperature-dependent total entropy in zero field and magnetic field H respectively, T_1 and T_2 are the lowest and highest temperatures respectively. Figures 7(a)–7(c) display the variation of $C_{\mathrm{p}}(0,T)$ with temperature for $La_{1.2}Fe_{11.6}Si_{1.4}C_x$ alloys. When $x = 0$, a sharp peak is obtained at 191 K, which is an indication of the FOMT. With increasing C content, the peak of $C_{\mathrm{p}}(0,T)$ shifts to the higher temperature, the value decreases gradually, and the shape be-

comes broader, owing to the weakened IEMT.[51] The temperature dependence of total entropy (S–T curves) in fields of 0, 1, and 2 T are exhibited in the inserts of Figs. 7(a)–7(c), and the ΔT_{ad} is evaluated from the horizontal (isentropic) distance between two S–T curves with and without magnetic field.[50] In principle, the decrease of specific heat capacity is beneficial to the increase of ΔT_{ad}. However, since the ΔS_M of $La_{1.2}Fe_{11.6}Si_{1.4}C_x$ alloys in this work is reduced with adding content of C, the ΔT_{ad}–T curve follows the same trend, as illustrated in Fig. 7(d). For $x = 0$, 0.25 and 0.5, the ΔT_{ad} are 4.90 K, 3.13 K, and 2.20 K under the field change of 2 T, respectively. The ΔT_{ad} of $La_{1.2}Fe_{11.6}Si_{1.4}$ and $La_{1.2}Fe_{11.6}Si_{1.4}C_{0.25}$ is higher than that of $La_{1.3}Fe_{11.6}Si_{1.4}$ ($\Delta T_{ad} = 1.49$ K and $T_C = 183$ K), $La_{1.7}Fe_{11.6}Si_{1.4}$ ($\Delta T_{ad} = 3.27$ K and $T_C = 184$ K),[50] and $LaFe_{11.1}Mn_{0.1}Co_{0.7}Si_{1.1}$ ($\Delta T_{ad} \sim 2.5$ K and $T_C \sim 252.5$ K)[52] with similar T_C. Furthermore, when $x = 0.25$ and 0.5, the ΔT_{ad} are comparable to the values of directly measured ΔT_{ad} for $LaFe_{11.6}Si_{1.4}C_{0.3}$ ($\Delta T_{ad} \sim 3.9$ K and $T_C \sim 244$ K) and $LaFe_{11.6}Si_{1.4}C_{0.4}$ ($\Delta T_{ad} \sim 2.5$ K and $T_C \sim 249$ K) under similar magnetic field change ($\Delta H = 1.9$ T).[44]

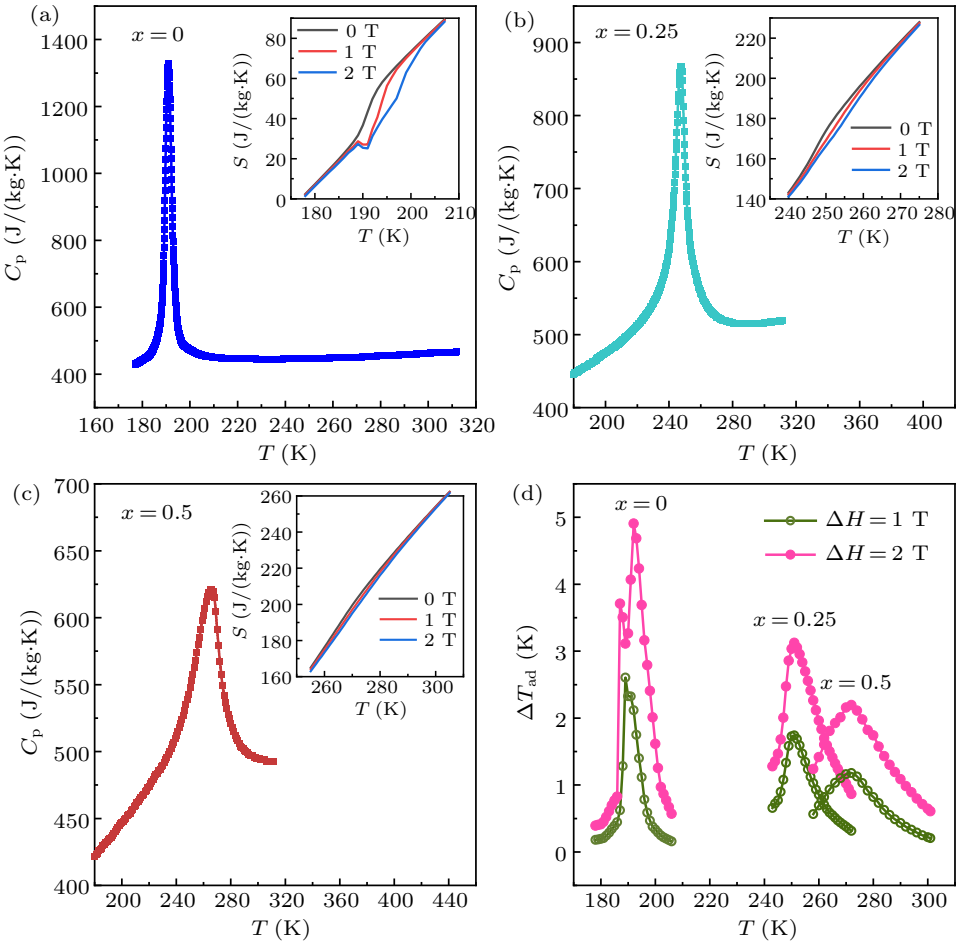


Fig. 7. (a)–(c) Temperature dependence of heat capacity under zero magnetic field for $La_{1.2}Fe_{11.6}Si_{1.4}C_x$ compounds, the insets show the S–T curves in 0 T–2 T magnetic fields. (d) The adiabatic temperature change as a function of temperature under field change of 1 T and 2 T.

4. Conclusion

The off-stoichiometric $La_{1.2}Fe_{11.6}Si_{1.4}C_x$ ($x = 0$, 0.25, 0.5, 0.75, 1) alloys were prepared by arc-melting and melt-spinning, and their microstructural, magnetic and magnetocaloric properties were studied. For the as-prepared samples, the primary and secondary phases in the C-free $La_{1.2}Fe_{11.6}Si_{1.4}$ alloy were identified as α-Fe and LaFeSi, respectively; while in the C-containing $La_{1.2}Fe_{11.6}Si_{1.4}C_x$ compounds, the C atoms tended to enter the LaFeSi lattice instead of the α-Fe lattice, generating the $La_2Fe_2Si_2C$ phase. The presence of C in $La_2Fe_2Si_2C$ inhibited the diffusion reaction and suppressed the formation of the 1:13 phase during the annealing process, although the intrusion of C refined the microstructure.

For the annealed samples, the C atoms occupied the 24d interstitial site in the 1:13 phase, resulting in the lattice expansion and raising the T_C from 192 K to 273 K. This also weakened the IEMT and shifted the magnetic transition from FOMT to SOMT, reducing the thermal and magnetic hysteresis significantly. Under the field change of 2 T, the $|\Delta S_M^{max}|$ decreased from 18.92 J/(kg·K) to 8.29 J/(kg·K) and 4.60 J/(kg·K), and the ΔT_{ad} decreased from 4.90 K to 3.13 K and 2.20 K, as $x$increased from 0 to 0.25 and 0.5, respectively. The $La_{1.2}Fe_{11.6}Si_{1.4}C_{0.5}$ alloy stands out due to its large mag-

netic entropy change, wide working temperature range and low cost compared to other magnetic refrigeration materials with similar T_C. These characteristics make it a promising candidate for near-room-temperature magnetic refrigerator technology.

Acknowledgements

Project supported by the National Natural Science Foundation of China (Grant No. 52272263), the University Synergy Innovation Program of Anhui Province, China (Grant No. GXXT-2022-008), the University Natural Science Research Project of Anhui Province, China (Grant No. 2024AH050145), the Youth Foundation of Anhui University of Technology (Grant No. QZ202303), and the National Innovation and Entrepreneurship Training Program for College Students (Grant No. 202310360018).

References

[1] Hou X, Lampen-Kelley P, Xue Y, Liu C, Xu H, Han N, Ma C, Srikanth H and Phan M H 2015 *J. Alloys Compd.* **646** 503
[2] Franco V, Blazquez J S, Ipus J J, Law J Y, Moreno-Ramirez L M and Conde A 2018 *Prog. Mater. Sci.* **93** 112
[3] Lyubina J 2017 *J. Phys. D: Appl. Phys.* **50** 053002
[4] Balli M, Jandl S, Fournier P and Kedous-Lebouc A 2017 *Appl. Phys. Rev.* **4** 021305
[5] Brown G V 1976 *J. Appl. Phys.* **47** 3673
[6] Pecharsky V K and Gschneidner K A 1997 *J. Magn. Magn. Mater.* **167** L179
[7] Wada H and Tanabe Y 2001 *Appl. Phys. Lett.* **79** 3302
[8] Li Z, Yang J, Li D, Li Z, Yang B, Yan H, Sánchez-Valdés C F, Llamazares J L S, Zhang Y, Esling C, Zhao X and Zuo L 2019 *Adv. Electron. Mater.* **5** 1800845
[9] Hu F X, Shen B G, Sun J R, Cheng Z H, Rao G H and Zhang X X 2001 *Appl. Phys. Lett.* **78** 3675
[10] Fan W B, Hou Y H, Ge X J, Huang Y L, Luo J M and Zhong Z C 2018 *J. Phys. D: Appl. Phys.* **51** 115003
[11] Zhang H, Hu F, Sun J and Shen B 2013 *Sci. China- Phys. Mech. Astron.* **56** 2302
[12] Gutfleisch O, Yan A and Müller K H 2005 *J. Appl. Phys.* **97** 10
[13] Chen X, Chen Y and Tang Y 2012 *Bull. Mater. Sci.* **35** 175
[14] Zhang H, Shen B G, Xu Z Y, Zheng X Q, Shen J, Hu F X, Sun J R and Long Y 2012 *J. Appl. Phys.* **111** 07A909
[15] Chen X, Chen Y and Tang Y 2011 *J. Alloys Compd.* **509** 2864
[16] Zheng H, Tang Y, Chen Y, Wu J, Wang H, Xue X, Wang J and Pang W 2015 *J. Alloys Compd.* **646** 124
[17] Barcza A, Katter M, Zellmann V, Russek S, Jacobs S and Zimm C 2011 *IEEE T. Magn.* **47** 3391
[18] Dai Y, Li Y, Xu Z, Luo Z, Han K, Zhai Q and Zheng H 2018 *J. Alloys Compd.* **765** 538
[19] Zhang H, Zhang X, Tan J, Yan J, Shi H, Zhang J, Wei H, Li H, Li W and Xia A 2023 *J. Alloys Compd.* **953** 170114
[20] Chen Y F, Wang F, Shen B G, Wang G J and Sun J R 2003 *J. Appl. Phys.* **93** 1323
[21] Liu X B, Liu X D, Altounian Z and Tu G H 2005 *J. Alloys Compd.* **397** 120
[22] Lyubina J, Gutfleisch O, Kuz'min M D and Richter M 2009 *J. Magn. Magn. Mater.* **321** 3571
[23] Liu J, He C, Zhang M X and Yan A R 2016 *Acta Mater.* **118** 44
[24] Li S, Huang R, Zhao Y, Wang W and Li L 2015 *Phys. Chem. Chem. Phys.* **17** 30999
[25] Song H, Hu Y, Zhang J, Fang J and Hou X 2022 *Materials* **15** 343
[26] Rodríguez-Carvajal J 1993 *Physica B* **192** 55
[27] Hüfken T, Witte A M and Jeitschko W 1998 *J. Alloys Compd.* **266** 158
[28] Boer F R de, Boom R, Mattens W C M, Miedema A R and Niessen A K 1988 *Cohesion in Metals: Transition Metal Alloys*, 2nd ed., January 1, 1989 (Amsterdam: North-Holland)
[29] Song W X and Zhao S J 2015 *J. Chem. Phys.* **142** 144504
[30] Fu S, Long Y, Sun Y and Hu J 2013 *Intermetallics* **39** 79
[31] Song B Y, Han Y Q, Cheng J, Gao L, Jin X, Sun Z B and Huang J H 2024 *J. Alloys Compd.* **990** 174398
[32] Liu J, Krautz M, Skokov K, Woodcock T G and Gutfleisch O 2011 *Acta Mater.* **59** 3602
[33] Zhang D, Wu Z, Li Y and Wang R 2022 *Coatings* **12** 534
[34] Chen Y F, Wang F, Shen B G, Sun J R, Wang G J, Hu F X and Cheng Z H 2003 *J. Appl. Phys.* **93** 6981
[35] Fujita A, Fujieda S, Fukamichi K, Mitamura H and Goto T 2001 *Phys. Rev. B* **65** 014410
[36] Fujita A, Fujieda S, Hasegawa Y and Fukamichi K 2003 *Phys. Rev. B* **67** 104416
[37] Chen Y F, Wang F, Shen B G, Hu F X, Sun J R, Wang G J and Cheng Z H 2003 *J. Phys.: Condens. Matter* **15** L161
[38] Phejar M, Paul-Boncour V and Bessais L 2010 *Intermetallics* **18** 2301
[39] Hashimoto T, Numasawa T, Shino M and Okada T 1981 *Cryogenics* **21** 647
[40] McMichael R D, Ritter J J and Shull R D 1993 *J. Appl. Phys.* **73** 6946
[41] Shamba P, Debnath J C, Zeng R, Wang J L, Campbell S J, Kennedy S J and Dou S X 2011 *J. Appl. Phys.* **109** 07A940
[42] Lin Z, Li S, Liu M, Duh J G, Peng K and Mao X 2010 *J. Alloys Compd.* **489** 1
[43] Chen X, Chen Y and Tang Y 2014 *Solid State Commun.* **186** 56
[44] Teixeira C S, Krautz M, Moore J D, Skokov K, Wendhausen P A P and Gutfleisch O 2012 *J. Appl. Phys.* **111** 07A927
[45] Law J Y, Franco V, Moreno-Ramírez L M, Conde A, Karpenkov D Y, Radulov I, Skokov K P and Gutfleisch O 2018 *Nat. Commun.* **9** 2680
[46] Debnath J C, Zeng R, Kim J H and Dou S X 2011 *J. Magn. Magn. Mater.* **323** 138
[47] Nadig P R, Murari M S and Daivajna M D 2024 *Phys. Chem. Chem. Phys.* **26** 5237
[48] Gottschall T, Skokov K P, Fries M, Taubel A, Radulov I, Scheibel F, Benke D, Riegg S and Gutfleisch O 2019 *Adv. Energy Mater.* **9** 1901322
[49] Engelbrecht K and Bahl C R H 2010 *J. Appl. Phys.* **108** 123918
[50] Kavitaa S, Alagusoundarya M, Ramakrishna V V, Suresh V, Bhatt P, Srimathi P, Archana R, Kar D, Thomas T and Gopalan R 2022 *J. Alloys Compd.* **895** 162597
[51] Lee A Y, Kang K H, Chung K C and Kim J W 2024 *Intermetallics* **173** 108408
[52] Abdulkadirova N Z, Gamzatov A G, Kamilov K I, Kadirbardeev A T, Aliev A M, Popov Y F, Vorob'ev G P and Gebara P 2022 *J. Alloys Compd.* **929** 167348